Journal of Environmental Management 345 (2023) 118833

Contents lists available at ScienceDirect

Journal of Environmental Management

journal homepage: www.elsevier.com/locate/jenvman

Research article

Development of rapid and effective oil-spill response system integrated with oil collection, recovery and storage devices for small oil spills at initial stage: From lab-scale study to field-scale test

Linfeng Piao [a], Chan Jin Park [a], Seongjin Kim [b], Kyungtaek Park [c], Yongjun Lee [d], Ho-Young Kim [a,e], Myoung-Woon Moon [b], Hyungmin Park [a,e,*]

[a] Department of Mechanical Engineering, Seoul National University, Seoul, 08826, South Korea
[b] Extreme Materials Research Center, Korea Institute of Science and Technology (KIST), Seoul, 02792, South Korea
[c] Korea Oil separate Assistance Institute (KOAI), Dong-eui University, Busan, 47340, South Korea
[d] Marine Environmental Control Equipment SEINPROTEK, Gimpo, 10064, South Korea
[e] Institute of Advanced Machines and Design, Seoul National University, Seoul, 08826, South Korea

ARTICLE INFO

Handling Editor: Raf Dewil

Keywords:
Integrated oil-spill response system
Oil separator
Oil storage tank
Hydrophilic surface structures

ABSTRACT

In the present study, through the laboratory-to-field scale experiments and trials, we report the development and evaluation of an integrated oil-spill response system capable of oil collection, recovery (separation), and storage, for a timely and effective response to the initial stage of oil-spill accidents. With the laboratory-scale experiments, first, we evaluate that the water-surface waves tend to abate the oil recovery rate below 80% (it is above 95% for the optimized configuration without the waves), which is overcome by installing the hydrophilic (and oleophobic) porous structures at the inlet and/or near the water outlet of the separator. In the follow-up meso-scale towing tank tests with a scaled-up prototype, (i) we optimize the maneuverability of the assembled system depending on the speed and existence of waves, and (ii) evaluate the oil recovery performance (more than 80% recovery for the olive oil and Bunker A fuel oil). Although more thorough investigations and improvements are needed, a recovery rate of over 50% can be achieved for the newly enforced marine fuel oil (low sulfur fuel oil, LSFO) that was not targeted at the time of development. Finally, we perform a series of field tests with a full-scale system, to evaluate the rapid deployment and operational stability in the real marine environment. The overall floating balance and coordination of each functional part are sustained to be stable during the straight and rotary maneuvers up to the speed of 5 knots. Also, the collection of the floating debris (mimicking the spilled oil) is demonstrated in the field test. The present system is now being tested by the Korea Coast Guard and we believe that it will be very powerful to prevent the environmental damage due to the oil spills.

1. Introduction

With increasing global awareness of the catastrophic damage caused by oil spills to the terrestrial and marine ecology and environment, responsive actions or efforts against the oil spills have attracted substantial attention of the public and media (Fingas, 2002). In general, the major marine oil spill refers to the accidental release of a huge volume of oil into the marine and/or coastal areas. A notable recent example is the Deepwater Horizon oil spill in 2010, with which nearly 800 million liters of crude oil were released into the Gulf of Mexico over three months (Barron, 2012); it subsequently caused a total economic loss of 8.4 billion dollars to commercial and recreational fishing industry alone (Sandifer et al., 2021). Once the oil spill occurs, the oil tends to spread fast along the free seawater surface in the form of a thin layer or a dispersed state (e.g., stable emulsion) (Fingas, 2002). It has been analyzed that the size and movement (e.g., spreading area and rate) of the oil in the marine environment, and the effect of weathering process (e.g., evaporation, dissolution, and dispersion) can influence the extent of subsequent damage (Alló and Loureiro, 2013; Dhaka and Chattopadhyay, 2021; Lee et al., 2023). Thus, it is critical to prevent the oil spill and/or to focus on the rapid and effective countermeasures for controlling and cleaning it up (Dhanak and Xiros, 2016; Fingas, 2016; Piao

* Corresponding author. Department of Mechanical Engineering, Seoul National University, Seoul, 08826, South Korea.
E-mail address: hminpark@snu.ac.kr (H. Park).

https://doi.org/10.1016/j.jenvman.2023.118833
Received 1 June 2023; Received in revised form 10 August 2023; Accepted 13 August 2023

et al., 2017; Piao and Park, 2019).

The effective countermeasure against the marine oil spills primarily aims to (i) prevent the oil from spreading to specific regions such as the shorelines and resources, (ii) to clean it up from the seawater, and (iii) to degrade any unrecovered oil; these processes are not separable but are preferentially operated in combination to minimize the impact on the marine environments (Dave and Ghaly, 2011). For example, the containment booms (so-called temporary floating barriers) are used to confine the spilled oil within the designated area and to make the subsequent cleanup and/or degradation processes easier. Depending on the spill size and cleanup techniques, different types of the booms like the fence-type, curtain-type, and fire-resistant booms have been used in the fields (Dave and Ghaly, 2011; Ossai et al., 2020). In addition to the confinement strategy, many techniques for direct cleanup and degradation of spilled oil have been developed to date, which can be broadly classified into four categories: mechanical recovery, chemical treatment, in-situ burning and biological remediation (Dhaka and Chattopadhyay, 2021). The mechanical recovery typically includes the oil skimmer and oil sorbent. The former recovers the floating oils from water through the skimming media (e.g., oleophilic belt, rope, and disk) or pump/suction mechanisms, while the latter is an insoluble, hydrophobic material (e.g., polypropylene) that is used to adsorb/absorb the oil phase (Dhanak and Xiros, 2016). Recently, overcoming the drawbacks of these devices such as low effective operation in severe environments (e.g., currents higher than 1 knot or wave height greater than 1 m) and secondary pollution induced by the oiled sorbent materials (Fingas, 2002; Dave and Ghaly, 2011), Lee et al. (2022a) developed a mechanical type oil recovery device (scooper) with a slippery, water-infusing membrane surface. This device allows only the water in the oil-water mixture to pass through and contain the oil phase on it, and it is currently successfully deployed into the fields for actual utilization (Lee et al., 2022b). Chemical treatment refers to the use of dispersants and solidifiers to alter the physical and chemical properties of the oil such that the modified chemical affinity for both oil (lipophilic) and water (hydrophilic) will reduce the interfacial tension between them; this leads to the breakup of the oil slick into tiny droplets which are easily degraded in the water column (Lessard and DeMarco, 2000; Dave and Ghaly, 2011). In-situ burning, as a thermal remediation method, is cited as an effective and viable response to oil spills (Dave and Ghaly, 2011; Dhanak and Xiros, 2016; Bullock et al., 2017). For the biological remediation, biodegradation agents such as hydrocarbon-degrading microorganisms, fertilizers, and other bio-stimulations are used to accelerate the natural degradation of petroleum hydrocarbons in marine environments (Si-Zhong et al., 2009; Fingas, 2016).

In practical applications of such devices, on the other hand, it is hard to determine the most effective countermeasures; each has its own advantages and limitations depending on the marine environment, weather condition, and the properties and thickness of the spilled oil slick. Or, some strategies involving the usage of chemicals are considered to have a harmful influence on the surroundings. For example, some less ecotoxic chemical dispersants have shown the potentials to effectively deal with the oil spills in a relatively harsh marine environment (e.g., high wind and strong waves) where most mechanical means are not properly working (Dave and Ghaly, 2011; Bejarano, 2018; Cai et al., 2021); however, their applicability is limited by the type of oil, sea-water temperature, and marine environment (Michel and Fingas, 2016). Ventikos et al. (2004) performed a compatibility analysis for remediation techniques/equipment based on the sea state, wind velocity, wave height, and oil properties, and provided the framework to determining the efficient oil response methods/equipment. They suggested that the combination of mechanical recovery and containment booms is the most common oil-spill countermeasure owing to its superior performance and friendly operability. By evaluating the advantages and disadvantages of various oil-spill response methods, Dave and Ghaly (2011) also suggested that the most effective cleanup is the incorporation of physical methods (e.g., booms and mechanical recovery) and bioremediation by dispersants. Following these analyses, on the other hand, recent studies have shifted their focus from existing (traditional) remediation techniques to developing new technologies for the early prevention and remediation to reduce the subsequent damage (Ivshina et al., 2015; Chen et al., 2019). In the same context, in the present study, we report the laboratory development and field deployment of the integrated oil-spill response system including a new mechanical type oil-water separator to achieve the timely and effective prevention, collection, and separation (oil recovery) at the early stage of the oil-spill accident. In the laboratory experiments, the roles of the porous hydrophilic structures installed at the inlet and/or the water outlet of the separator on the oil recovery performance under wave conditions were tested to enable our system to reliably run in the actual marine environments. With the meso-scale towing tank flow tests, the maneuverability of the assembled system (in real scale) was evaluated while varying the speed and wave condition of the flow, and we examined the viability of oil collection, recovery, and storage with the actual fuel oils. Finally, we performed the field-scale trials to primarily assess the operational stability (e.g., floating balance and sturdiness of connection between each component) of the entire system at different towing speeds and movements. Also, we confirmed the recovery performance of the system with floating debris mimicking the oil slick. The present system is now deployed to the field and being tested by the Korea Coast Guard, and we believe that it will have a great impact on the fast and efficient response to the oil-spill accidents, especially dealing with small oil spills at the early stage of the accident.

2. Conceptualization: Integrated oil-spill response system against the marine oil spills

Herein, we explain the operational and functional concepts of the present integrated oil-spill response system for the rapid and effective prevention and remediation at the initial stage of the oil-spill accident (Fig. 1). As shown, the present system is basically the mechanical type, being comprised of the oil containment boom/fence, oil-water separator, oil storage tank, and vane deployer. When the system is dispatched to the site of oil spills, the assembled system is in principle driven (towed) by a single small offshore boat (e.g., fishing boat) with the assistance of the vane deployer (or so-called guide vane) that was developed to maintain the propulsive performance without the sudden drop in the lift-to-drag ratio during maneuvering at wide range of incidence angles (Park and Park, 2019).

The oil containment boom/fence is used to collect and force the oil slick to flow into the oil-water separator. The oil-water separator is a novel oil-recovery device developed by the authors and colleagues (Piao et al., 2017; Piao and Park, 2019), which is a mechanical device based on the gravitational effect (Behin and Azimi, 2015). Once the influx of oil-water mixture is first guided downward along U-shaped curved path, the kinetic energy increased by being accelerated is transferred to the potential energy as the mixture rises over an uphill. During this process, the phase separation happens after the flow passes the gap below the baffle plate (see Fig. 2b) and the separated oils climb up along the backside of the baffle plate. When the accumulated oil layer becomes larger than the critical volume, they flow over the weir plate and into the storage tank with the assistance of a portion of the water layer below (see the inset of Fig. 3c); on the contrary, the excess water is released out of the separator through the water outlet at the bottom of the separator. This mechanism of the oil-water separator has been confirmed numerically by Piao et al. (2017), and the experimental demonstration and theoretical analysis of the oil-water interfacial flow associated with the oil recovery were done by Piao and Park (2019). It is worth noting that the present separator can process the oil-water mixture flow continuously by intensifying the effect of phase separation driven the density difference through the U-shaped channel (adding centrifugal acceleration to the gravitational acceleration).

When accidental oil spills occur offshore, it is a general procedure to

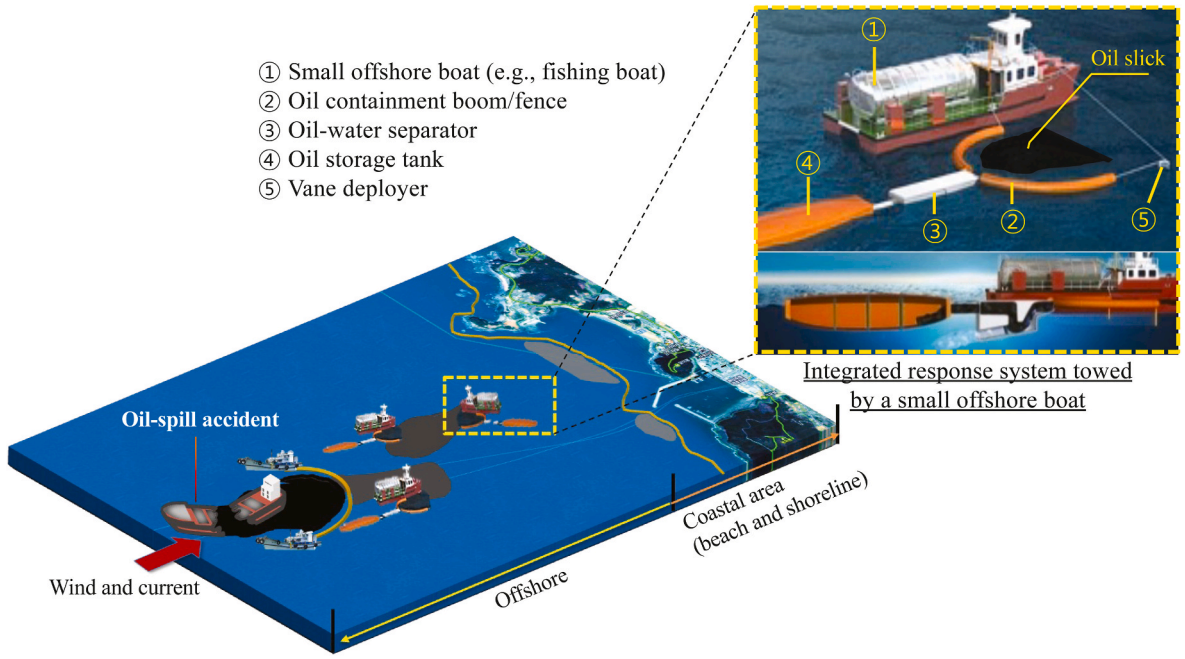

Fig. 1. Schematic diagram to illustrate the concept of the present integrated response system against the oil-spill accidents, which is composed with the oil separator, oil containment boom/fence, oil storage tank, and vane deployer. Here, darkness level of the oil slick represents its relative thickness on the water surface.

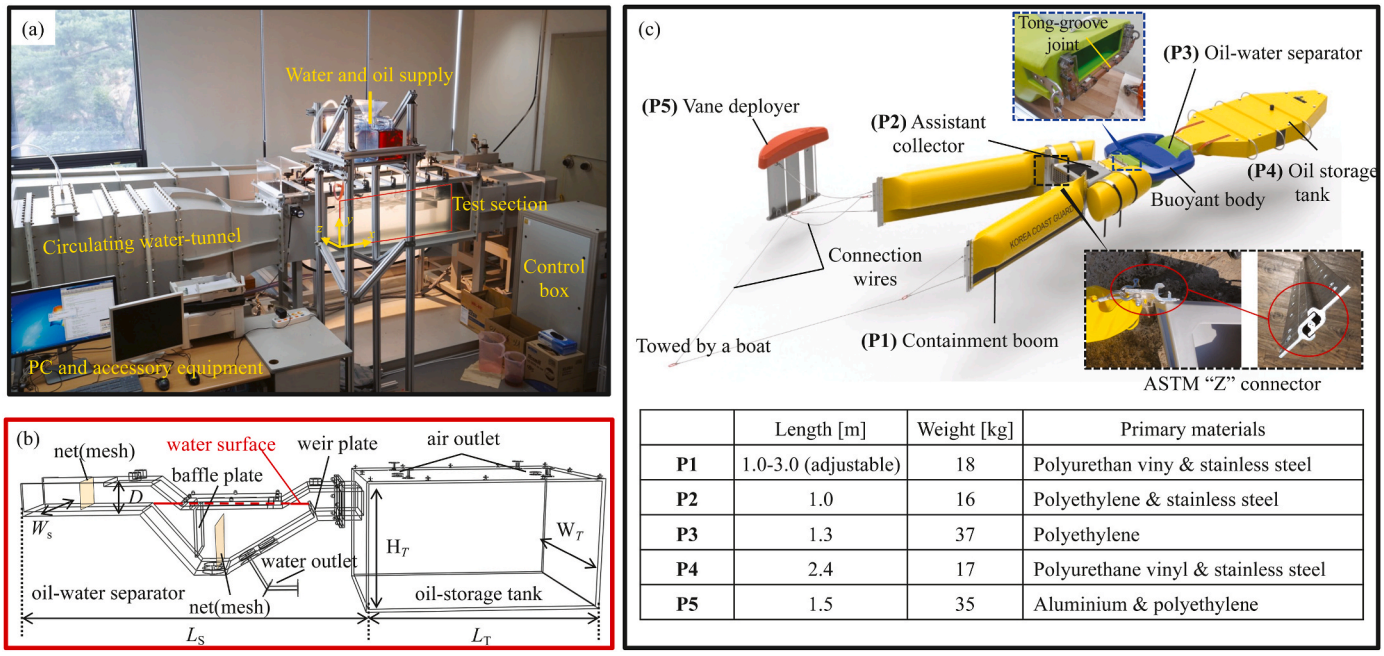

	Length [m]	Weight [kg]	Primary materials
P1	1.0-3.0 (adjustable)	18	Polyurethan viny & stainless steel
P2	1.0	16	Polyethylene & stainless steel
P3	1.3	37	Polyethylene
P4	2.4	17	Polyurethane vinyl & stainless steel
P5	1.5	35	Aluminium & polyethylene

Fig. 2. Description of the present integrated response system considered for different flow tests: (a) lab-scale version tethered in the large-scale circulating water tunnel; (b) detailed configuration of the lab-scale oil-water separator and oil storage tank; (c) scale-up version of the system used for towing tank and field tests (Image credit: KOAI Co., Ltd.).

deploy the containment boom encircling the accident area to prevent spreading (Fig. 1). However, the delayed deployment or failure of the fence will cause the oil spreading towards the coastal area driven by the wind and current (Fingas, 2002; Ventikos et al., 2004). It is clear that the economic damage and cost for cleanup will increase significantly once the oil reaches the beaches and shorelines (Dhaka and Chattopadhyay, 2021). Considering the limitations of conventional oil skimmers at the early stage of oil spills (for example, when oil spreading is faster than the speed of skimming), we suggest that the multiple systems are operated together, of which each is towed by small offshore boats such that the mobility of the operation can be maintained for tackling early, small oil spills, without the specialized cleanup ships, as illustrated in Fig. 1. The overall length and storage capacity of the proposed system are ~ 10 m and ~ 1000 L, respectively, to ensure the lightweight, easy assembly and deployment, and low towing drag, for enhanced mobility. The easy replacement of the storage tank may allow the system to be operated continuously despite its limited storage capacity. For instance, the professionals (e.g., coast guards) can easily replace the full storage tank with a new one and continue the operation. As show in Fig. 1, it will allow the multiple deployments and fast operations to tackle the

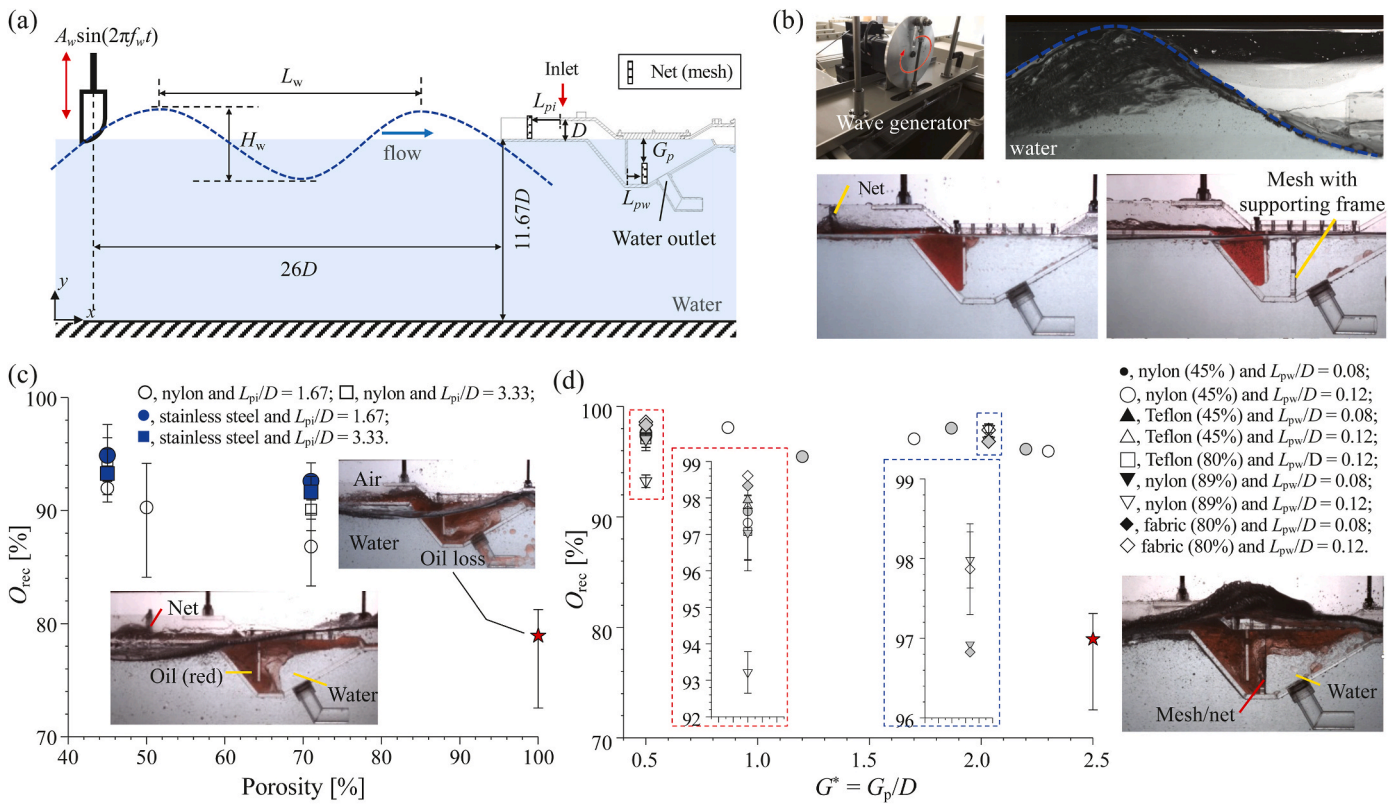

Fig. 3. Surface waves test in lab-scale experiments: (a) wave generation depending on the forcing amplitude (A_w) and frequency (f_w) of the generator; (b) picture of typical waveform (top) and instantaneous oil-water flow structure in the oil-water separator with a net at the inlet (bottom left) and a mesh near the water outlet (bottom right); (c) variation of O_{rec} with the porosity of the porous structures located at the inlet, according to the wettability and location (L_{pi}); (d) variation of O_{rec} with $G^* = G_p/D$ between the top wall and porous structure near the water outlet. The reference case (without the mesh/net) in (c) and (d) is represented with ⋆.

early-stage oil spills.

In the following, we will discuss the feasibility and validity of the proposed system to collect, recover, and store oil slicks from the water surface rapidly and successfully based on laboratory-to-field scale experiments and trials. It is noted that a complete assessment on the functionalities of the system such as the quality of water released out of the separator and the effects on the marine ecological environments is beyond the scope of the present work and will be reported once the field evaluations are done by the Korea Coast Guards.

3. Equipment, materials, and methods

3.1. Integrated oil-spill response system for flow tests

In the present study, we used the prototypes with two different scales according to the size of flow facility. First, the lab-scale oil-water separator (and the storage tank) is used for the flow test in the large-scale circulating water tunnel, of which the test section is 1500 mm × 400 mm × 500 mm in the streamwise (x), vertical (y), and spanwise (z) directions, respectively (Fig. 2a). As shown in Fig. 2b, the width and length of the oil-water separator is $W_s = 3D$ and $L_s = 15D$, respectively, and the volume of the oil storage tank is $210D^3$, where D (= 30 mm) is the height of the inlet of the separator. With this setup, we evaluated the oil recovery (separation) rate of the present oil-water separator under the surface wave conditions and also tested the effect of supporting parts (e.g., porous structures) on the mitigation of the performance degradation by surface waves. Note that in our previous studies that considered the same geometry of the separator, the effects of waves and the associated countermeasures were not investigated. The properties of the tested porous structures are summarized in Table 1. Owing to the limited size of the water tunnel, the separator was tethered such that the position of the water surface is aligned to the horizontal level of the end of the weir plate (see red line in Fig. 2b or Fig. 3a), which was found to be an optimal position to maximize the separation performance (Piao et al., 2017; Piao and Park, 2019). The water flow (including the oil) was introduced at the speed of 0.1–2.0 m/s. The geometrical details of the flow facility and the separator such as the baffle plate, weir plate, and water outlet can be found in previous studies (Piao et al., 2017; Piao and Park, 2019).

Table 1
Specifications of the porous structures used in the laboratory-scale wave tests. Here, the fabric composed of microfibers was treated by the oxygen plasma to have the superhydrophilic property (Lee et al., 2022a).

Location	Materials	Wettability	Pose size [mm]	Porosity [%]
Inlet	Nylon	Hydrophobic/ oleophilic	1–4	45, 50, and 70
	Stainless steel	Hydrophilic/ oleophilic	1	45 and 70
Water outlet	Teflon	Hydrophobic/ oleophilic	0.75–1	45 and 80
	Nylon	Hydrophobic/ oleophilic	1–4	45 and 89
	Special fabric	Superhydrophilic	0.15	12–25

In meso-scale towing tank and field tests, on the other hand, we used the scale-up version of the entire system, which is composed of the containment boom (with the assistant collector), oil-water separator, oil storage tank, and the vane deployer (Fig. 2c). The length of the entire system is approximately 10 m, and the height of separator inlet (D) is 5 times larger than that of the separator used in the lab-scale experiments. In addition to the containment boom, the assistant collector (which was

not considered in the water-tunnel tests) is considered to minimize the boom failures from drainage and/or critical accumulation (Fingas, 2002). Unlike the laboratory-scale tests with the separator and tank tethered, the outer profile of the oil storage tank was newly designed to reduce the drag force applied during the maneuvering in the ocean. While the maximum volume of the tested system is approximately 1000 L, it can be flexibly varied according to the demand. For the fast and easy deployment of the system in real environments, we ensured that each component has a relatively light weight, and they are connected (assembled) through the ASTM "Z" connector and tong-groove joint. As explained in Fig. 2c, polyethylene (PE) is the main material considered for its lightweight, easy-to-clean impact and corrosion resistance, while polyurethane vinyl fabric, stainless steel frames, and aluminum plates are used for their high tensile strength and adaptability (e.g., customized shaping and foldability), to ensure the durability and chemical resistance of the system in the marine environment. In the below, we will explain more details on each flow test with different scales and purposes.

3.2. Laboratory-scale experiments for advancement of oil-water separator

A series of laboratory-scale experiments for the oil recovery were conducted under the surface wave conditions in the circulating water tunnel (Fig. 2a). The wave generator, located at 26D in front of the inlet, is designed to produce the surface waves periodically by controlling the forcing.

Amplitude (A_w) and frequency (f_w). The resultant height (from trough to crest, H_w) and wavelength (L_w) of the waves vary from 1.0D−5.0D and 10D−28D, respectively, for the range of flow speed considered (Fig. 3a). Like the oil recovery measurement (without the surface waves) reported by Piao and Park (2019), we supplied the oil and water together through the inlet of the separator that is tethered at the top of the test section. For the present experiments, silicone oil was used, of which the density and kinematic viscosity is 935 kg/m^3 and 10 mm^2/s, respectively. The volume flow rate of oil and water measured at the separator inlet is fixed as Q_o = 70 mL/s and Q_w = 12 mL/s, respectively, and the wave height was controlled to be as high as 5D.

While evaluating the effect of surface waves on the performance of oil separator, we also tested the mitigation of the surface wave effect by installing the porous structures of net and mesh at the separator inlet and water outlet, respectively (Fig. 3). The net is installed at a distance of L_{pi}/D (= 1.67 − 3.33) from the inlet, of which the pore size and wire diameter are 0.75–4.0 mm and 0.25 − 1.0 mm (see Table 1), respectively, is expected to play the role of wave (or ocean current) damper, while the superhydrophilic mesh at the water outlet is applied to directly prevent the oil loss through water outlet due to the fluctuating flows inside the separator caused by the interfacial instability (e.g., interfacial fluctuation and dispersed oils) (Piao and Park, 2019, 2021). We controlled the location (L_{pw}) and the gap (G_p) between the top wall of the separator and porous structures erected near the water outlet as 0.08D − 0.12D and 0.5D − 2.5D, respectively (Fig. 3a). Here, we investigated the effect of wettability, pore size, and porosity of porous structures on the oil recovery rate. For each experiment, we measure the supplied (V_{so}) and recovered oil volume (V_{ro}), and calculated the oil-recovery rate as $O_{rec} = V_{ro}/V_{so}$. After each oil recovery test, we measured V_{ro} after leaving the tank for a while (e.g., more than 24 h), by which the separation line between the oil and water was identified clearly. At the same time, we also visualized and analyzed the oil-water interfacial patterns inside the separator, using the same experimental setup used in Piao and Park (2019).

3.3. Towing-tank experiments for evaluating the maneuverability and oil recovery

We performed a series of towing-tank experiments with the prototype system of the same scale as the real product. Depending on the purpose (or the permission to use the actual fuel oil at the site), tests were done at two different flow facilities. First, for the purpose of checking the maneuverability of the entire system with the waves, we used the Seoul National University Towing Tank (SNUTT), of which the length, width, and depth is 100 m, 8 m, and 3.5 m, respectively. The maximum towing speed is 5 m/s (9.72 knots) and the waves generated in the tank has length of 0.25–6.25 m, period of 0.4–2.0 s, and height of 0–0.3 m (Park et al., 2022). In the present study, we considered the fixed towing speed of 3 knots, which is a normal operating condition in a real marine environment. Then, under the given conditions of the period of 2 s and wavelength of about 6.0 m, we examined the effects of the height of surface waves (0.15 m and 0.3 m) on the floating balance and the performance of unfolding the containment boom during maneuvering.

On the other hand, the evaluation of the oil collection, recovery, and storage using the scale-up version of the present system was carried out in the towing tank facility (33 m in length, 24 m in width, and 2.6 m in depth) located at the Yeosu Korea Coast Guard Academy. The facility is featured by the towing speed up to 1.03 m/s (2.0 knots), generation of the surface waves, and most importantly the utilization of various fuel oils. We tested Bunker A fuel oil and olive oil, but also a new low sulfur fuel oil (LSFO, SK innovation Co., Ltd) that was very recently enforced to use mandatorily by the International Maritime Organization (IMO) (Lee et al., 2022b, 2023). The Bunker A is a member of the bunker fuel oil family (Uhler et al., 2016; Schnurr and Walker, 2019), which is a mixture of light fuel oils (diesel) and heavy fuel oils in a ratio of 7:3. Owing to its features such as low viscosity and low content of residual carbon, it is often used as a fuel oil for media/small marine vessels and home heating. Note that the LSFO was not mandated at the time of developing and testing the present oil-recovery system; however, it is found that the present development shows a reasonably upstanding performance against the LSFO (see below). In Table 2, we have provided the relevant properties of the tested oils. Here, instead of using the vane deployer, the response system was attached to the towing carriage via the aluminum supporting frame (Fig. 4a) and translated at the speed of 2.0 knots. While continuously releasing the target oils on the water surface during towing, we recorded the oil flow patterns near the containment boom (Fig. 4b), and also monitored the entire test procedure and oil-water mixture flow through the storage tank using the mobile camera and action camera (Go Pro black 8), respectively. After the flow testing, we measured the volume of recovered test oils (Fig. 4c) and calculated the oil recovery-rate (O_{rec}) that is defined as same as the water-tunnel experiments.

3.4. Field-scale trials for deployment and operation in marine environments

After we have confirmed the performance of the present system through the series of in-door flow tests, finally we performed several field-scale trials at different ports around the Korea coast for the evaluation of the rapid deployment and operational stability of the entire scaled-up system. The ports we have tested are Pyeongtaek, Mokpo, and Busan, located along the west and south coast of Korea. The average wind speed and wave height on the sea varied in the range of 1.5–5.0 m/s and 0.1 − 0.5 m, respectively, depending on the season and locations. As shown in Fig. 4d, the entire response system was easily assembled by 3–4 persons on the ground (or on the ship deck) within 10–20 min before being deployed at sea. Together with the vane deployer, the response

Table 2
Properties of the oils used in the meso-scale towing-tank experiments.

Properties	Olive oil	Bunker A fuel oil	LSFO
Density at 15 °C [kg/m^3]	919	800–900	920
Kinematic viscosity at 50 °C [mm^2/s]	$\lesssim$ 38	$\lesssim$ 20	380
Pour point [°C]	$\lesssim$ 3	5	17
Flash point [°C]	210	$\gtrsim$ 60	148
Sulfur content [wt%]	N/A	2	0.47

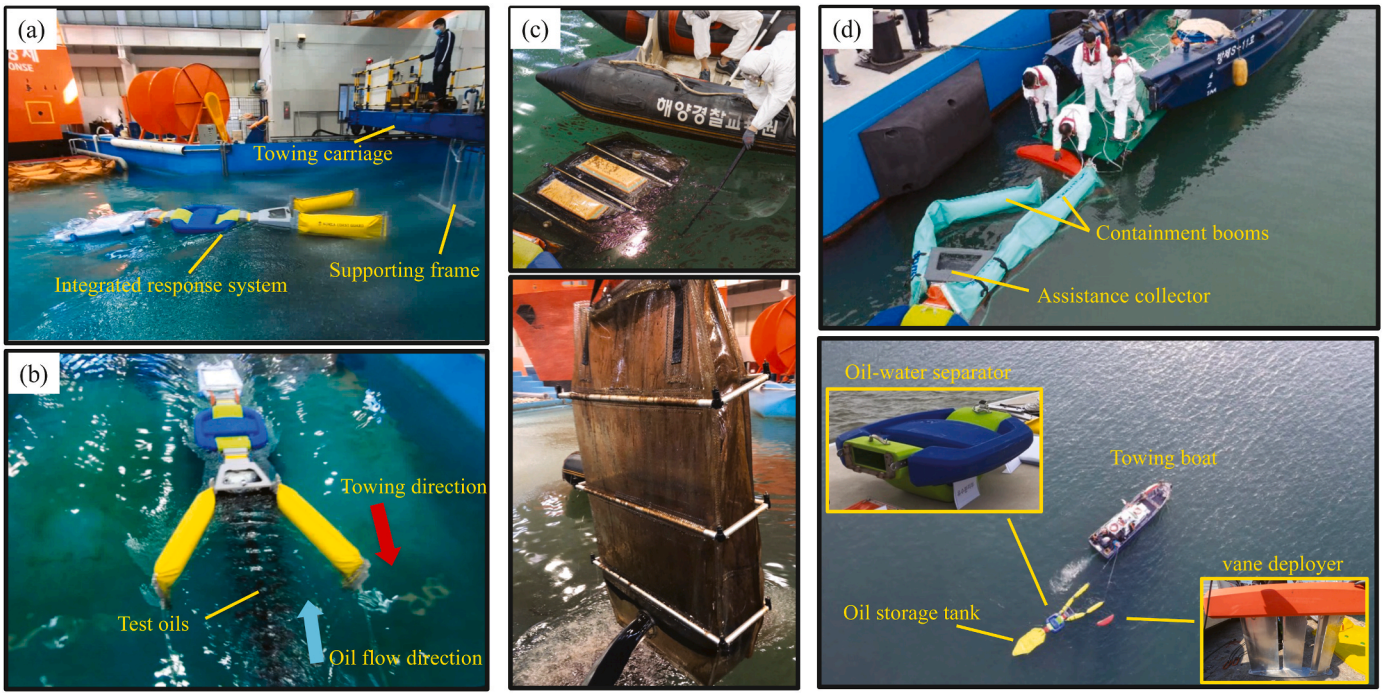

Fig. 4. Evaluation of the system performance with the scaled-up integrated response system: (a) meso-scale towing tank tests for oil recovery; (b) oil collection and recovery in towing tank tests; (c) measure of the oil recovery; (d) field-scale trials at different ports around the Korea coast.

system was towed (operated) by a single small boat, for example, a 10−ton surveillance boat of the Korea Coast Guard or a 2.55−ton private fishing boat. For each test, we set the towing speed in a range of 1.0–5.0 knots (0.51 − 2.57 m/s) and examined the operational stability under the different towing motions, such as linear and rotary movements. To record the whole operating situation, we used drone aerial photography technologies for multi-angle views (Fig. 4d). In addition to the assessment of operational stability, we used the color foam balls (i.e., floating debris) with a diameter of 20–30 mm at the Coast Guard exclusive port area (ensuring that the missing foam balls are in the controlled region for easy subsequent recovery) to mimic the oil spill in a real marine environment, aiming to examine the capability of the system for collecting and recovering spilled materials. We tracked the floating debris using the different angled drone cameras and used the action camera installed on the assistant collector to capture the motion of floating debris near the inlet.

4. Results and discussion

4.1. Porous structures on mitigating wave effects

In our previous study (Piao and Park, 2019), it was well explained that the highly agitated high-speed flow of the oil-water mixture into the separator causes the fluctuating oil-water interface and dispersed oil phase (interface breakup) inside the separator, which are associated with the degradation of the oil recovery (i.e., loss of oil). Thus, it is expected that the surface waves in the harsh environmental situation would be detrimental to maintaining the successful oil recovery and separation of the present system. To cope with such cases, we compared the effects of the porous structures located near the separator inlet and/or water outlet, which are considered as a kind of wave (or ocean current) damper and/or to keep the stable water layer under the oil to be separated, respectively. As expected, without any countermeasures, it is measured that the surface waves decrease the oil-recovery rate noticeably (refer to star symbols in Fig. 3c and d, and the typical instantaneous flow pattern is shown on the right top in Fig. 3c); for example, the wave with a height of 5D decreases O_{rec} below 80% (92 − 98% without waves) at the given flow condition of Q_o = 70 mL/s and Q_w = 12 mL/s. The variation of O_{rec} with the porosity of the net located near the separator inlet and the typical flow pattern of the oil phase inside the separator are shown in Fig. 3c. In addition to the porosity and material (wettability) of the net (see Table 1), we tested different locations as L_{pi}/D = 1.67 and 3.33. The vertical bar of each data point in Fig. 3c denotes the range of data scattering from repeated measurements. Compared to the reference case without the net (i.e., 100% porosity in Fig. 3c), it is clear that the oil-recovery rate of the separator with the net is enhanced; O_{rec} increases gradually with decreasing the porosity and recovers O_{rec} of 95% for the porosity of 45%. The location and wettability of the net have negligible influences on O_{rec} for the relatively low porosity of structures but, interestingly, the wettability affects the impact of location on O_{rec}. For instance, at a given porosity of 70%, the hydrophilic net (stainless steel) installed at L_{pi}/D = 1.67 results in the higher O_{rec} than that installed at L_{pi}/D = 3.33; however, for the hydrophobic net, O_{rec} shows the opposite trends. This is because the additional hydrophilic feature of relatively low flow-resistant to the water phase helps keeping the stable water layer under the oil phase near the water outlet in addition to the wave-damping role of the net, which may provide a useful guideline to devise this kind of wave damping porous structure in marine application. The typical flow patterns of the oil phase inside the separator reveal that the oil loss under wave conditions (see the inset figure of Fig. 3c) is strongly related to the interfacial fluctuation inside the separator (Piao and Park, 2019), which is not observed when the net is installed (see the inset of Fig. 3c).

Next, we investigated the variation of the oil-recovery rate with the gap (G^* = G_p/D) between the top wall of the separator and porous structures erected near the water outlet while varying its wettability (e.g., nylon, Teflon and fabric), porosity (45−89%), and the location (L_{pw}) (Fig. 3a and d). With this device, we aim to directly suppress the fluctuating oil-water interface inside the separator while keeping a stable water layer above the water outlet, which was revealed as the key flow feature to successfully separate the oil from the mixture (Piao et al., 2017; Piao and Park, 2019). As shown in Fig. 3d, the existence of the net next to the baffle plate inside the separator enhances the oil-recovery rate beyond 90% (96% in average). In particular, for the nylon net

with a porosity of 45%, O_{rec} as high as 98% can be achieved even changing G^*. When G^* is fixed as 0.5, except for the case of the fabric net, O_{rec} decreases as the porosity increases at the given L_{pw}. It is noted that the effect of the location is ignorable (less than 1% in O_{rec}) as the porosity goes below 80%, but for the nylon net with the porosity of 89%, O_{rec} becomes higher at $L_{pw}/D = 0.08$ than that at 0.12 (highlighted with the red dashed box in Fig. 3d). This is attributed to the higher porosity (>80%) that tends to lose the suppressing effect of the mesh/net on the interfacial fluctuation near the water outlet. The maximum enhancement ($O_{rec} = 98.6\%$ at $G^* = 0.5$) of the oil-recovery rate was achieved with the fabric net treated by oxygen plasma to be superhydrophilic (Lee et al., 2022a). At $G^* = 2.0$, however, both nylon and fabric nets result in the higher O_{rec} at $L_{pw}/D = 0.12$ than that at 0.08 (marked by the blue dashed box in Fig. 3d). With the mitigated wave effect, it is also confirmed that the oil-water interface becomes quite stable over the water layer inside the separator, as shown in the bottom inset figure in Fig. 3d. The results of laboratory-scale experiments have shown that the negative effect of surface waves can be effectively mitigated by installing porous structures in the separator. We believe that the combination of these approaches would allow the present system to operate reliably in harsh marine conditions.

4.2. Maneuverability of the assembled system

As shown in Fig. 2c, we scaled up the oil-water separator optimized for the laboratory-scale study and assembled it with other functional components such as the vane deployer, containment boom, assistant collector, buoyant body, and the oil storage tank. To check the maneuverability of this assembled system, we focused on testing the floating balance and the performance of unfolding mechanism of containment boom with the assistance of the vane deployer. Shown in Fig. S1 in the Supplementary Materials are temporal movements of the assembled system during maneuvering in the towing tank, of which the wave heights are 0.15 m and 0.3 m, respectively, with a wavelength of about 6.0 m and a period of 2 s. For both tests, t = 0 s represents the moment after the system is deployed on the water surface and before it is towed. After towing, this system will have the same speed, 3 knots (1.54 m/s) as the towing carriage. When the surface waves in the towing tank is mild, (wave height of 0.15 m), the fully unfolded state of the containment boom is achieved after 10 s, which is sustained stably until the towing test stops (Fig. S1a; for details, see supplementary movie S1). This shows that the present system works well achieving a stable floating balance and fast unfolding characters of the boom even in the situation with surface waves. The same capability was confirmed when the wave height increases to 0.3 m (Fig. S1b). Considering the acceptable maneuverability of this system, we will extend its relevant assessment to field-scale tests in section 4.4.

4.3. Oil collection, recovery, and storage for the scaled-up response system

Here, we discuss the operational functionalities of the scale-up version of the present system, identified during the towing-tank experiments such as the oil collection, recovery, and storage. According to laboratory-scale tests, in order to maintain the prominent oil-recovery rate with the scale-up version, we learned that (i) the oil slick should be collected toward the inlet, (ii) the drag on the oil flow needs to be reduced, and (iii) the proper inflow of water is needed to maintain the water layer above the water outlet (Piao et al., 2017; Piao and Park, 2019). This requires the optimization of the collection system as well as the controllable water level at the inlet of the separator. As shown in Fig. S2 in the Supplementary Materials, we tried to evaluate different types of the connection mechanism between the containment barrier and assistant collector, i.e., the separation type (Fig. S2a) and combination type (Figs. S2b and c). The former provides easy and fast connection between the containment boom and the assistant collector via the ASTM "Z" connectors (Fig. 2c) but the latter ensures the separator, the assistant collector, and the containment boom integration to keep a relatively stable floating balance and maintain the water level at the proper position. While the separation type has a better oil collection functionality (see Fig. 4a), we found that it shows a relatively higher flow resistance acting on the oil-water mixture inflow causing the critical accumulation failure of the containment boom (Fingas, 2002). The combination type, on the other hand, can achieve a sort of floating balance of the height between the separator inlet and the collection system by controlling the bulk density of the buoyant bodies. When a small portion ($\lesssim 0.1D$) of the separator inlet is immersed under water, which is similar to the experimental setup of the tethered separator in the water-tunnel experiments, the floating balance is optimized to allow the collected oil to flow into the separator smoothly with the assist of inflow water while maintaining the water layer above the water outlet. If necessary, the length of the containment boom can be changed to reduce the weight of the system (Fig. S2c). Fig. S2d depicts the easy assembly process using tong-groove joints; i.e., a person can assemble the separator and assistant collector (already combined with the containment boom) when another person holds the assistant collector on one side.

The most important check point is to confirm that the similar level of the oil recovery is achieved with the scale-up version of the system while being towed. Fig. 5a compares the oil-recovery rate of the scale-up version of the integrated oil-spill response system measured in the towing-tank tests with that of the laboratory-scale separator in the circulating water-tunnel tests. Although the oil was released in different ways in the laboratory-scale and towing-tank tests, the oil-water mixture inflow rate was measured to be similar to each other as the towing speed of 1.03 m/s (2.0 knots). During the oil-recovery tests, we observed that separated oil is safely stored in the storage tank, of which the surface is made to be transparent intentionally (Fig. 4c). As shown in Fig. 5a, the oil-recovery rates of the Bunker A fuel oil and olive oil were measured to be 80% and 83.3%, respectively, in the towing tank tests, which are close to the averaged recovery rate (85.8%) of the silicone oil measured in the laboratory-scale experiments. This demonstrates that the scaled-up integration response system has a reliable oil recovery performance and works well for various oils with relatively low viscosities (see supplementary movie S2).

While the present system shows an excellent performance against the originally targeted fuel oils, the oil-recovery rate drops to 50% for the low sulfur fuel oil (LSFO), a new generation marine fuel oil (see Table 2), under the same test condition. Considering that this rate may underestimate the actual performance because most LSFO was observed to stick to the walls of the collector and separator due to its higher viscosity (Fig. 5b), we think this is a quite encouraging result. Lee et al. (2022b, 2023) reported that the adhesion behavior of the LSFO is attributed to the solidifying viscous properties elevated at the relatively low temperatures; however, our understanding to date is still insufficient. To our best knowledge, this is the first time to cope with the meso-scale spill of the special LSFO using the mechanical type of the separator. Furthermore, we are also currently working on developing novel devices specified for collecting the LSFO with higher viscosity.

4.4. Rapid deployment and operational stability in marine environments

So far, the results of the laboratory-scale and towing tank tests have clearly shown that the present integrated oil-spill response system can recover the oil slicks on the water surface reliability and effectively under wide range of conditions. We now turn to the analysis on the feasibility of its rapid deployment and stable operations in the real marine environment. Fig. 6a–c exhibit the exampled photographs taken during the maneuver of the full-scale integrated response system towed by a small boat and vane deployer (see supplementary movie S3). In the field-scale trials, the curtain-type containment barriers were used instead of the simple booms, and also the vane deployer with multiple

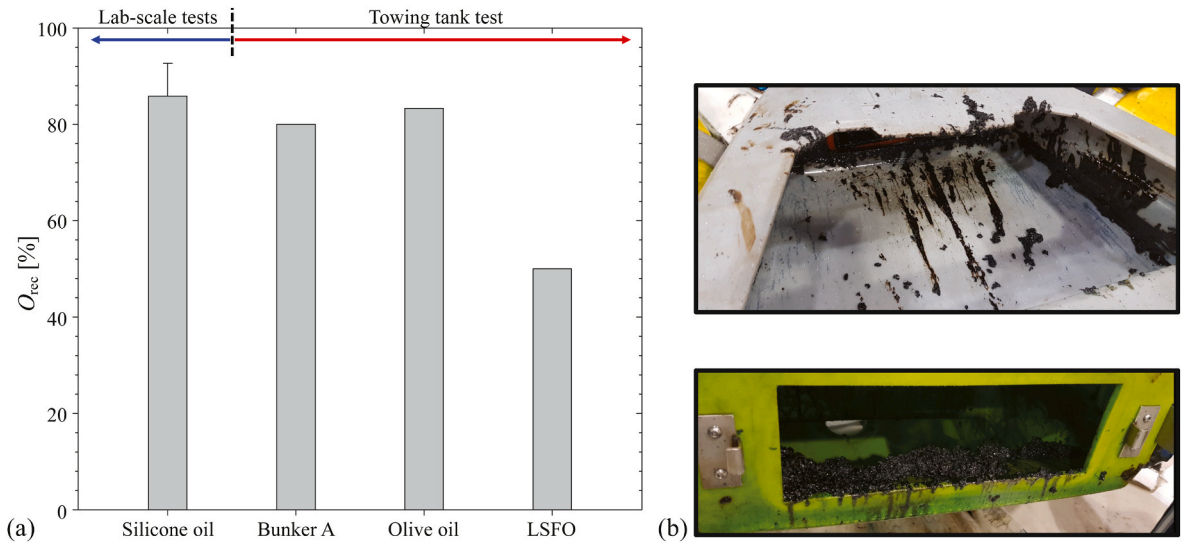

Fig. 5. (a) Comparison of the oil-recovery rate achieved in the laboratory-scale experiments and meso-scale towing tank tests of the scaled-up integrated response system. (b) Residue of the LSFO, owing to the higher adhesive property and viscosity, in the system after the flow tests.

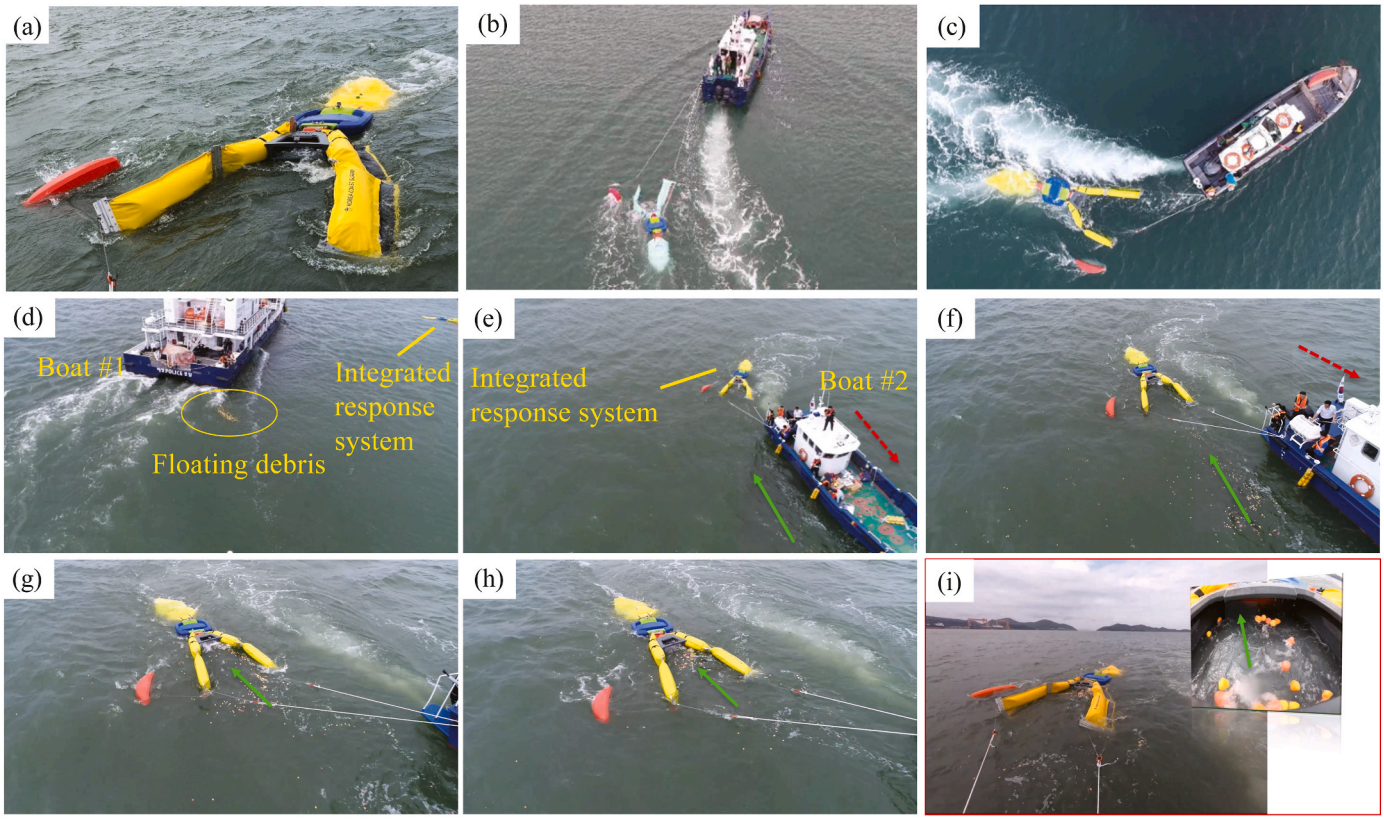

Fig. 6. Performance assessment of the integrated oil-spill response system in field-scale trials: (a–c) stable operation (at the speed of 1.29 m/s) of the integrated response system driven by a small boat and a vane deployer. Here, the containment boom has the underwater curtain; (b–c) Linear and rotational movements of the system at the speeds of 3–5 knots; (d–h) sequential tracking of the floating debris (colorful foam balls) through drone cameras; (i) motion of floating decries near the inlet captured by the action camera. Here, the green solid and red dashed arrows represent the primary direction of the movement of floating debris and the direction of the towing boat #2, respectively. The towing speed is 2.5 knots.

hydrofoils was used like the towing tank tests (Park and Park, 2019). Each component of the present system weighs less than 20 kg and is assembled with a simple detachable design (e.g., ASTM "Z" and tong-groove connectors), which greatly reduces the loading (unloading) time and the manpower input required for the assembly (see Fig. 2c). Moreover, combined with the capability of the present separator to treat different oils (reducing the time spent on selecting viable equipment for special oil types), we found this significantly saves the total deployment time that is critical for fast prevention and cleanup at the early stage of oil-spill accidents. As the importance of floating balance to the successful oil recovery was highlighted in the towing tank tests, we also examined the operational stabilities, e.g., the floating balance and the

sturdiness of the connection between each part during various maneuvering modes. As shown in Fig. 6b and c, for example, the total system still shows a stable operation during the rotational movement at the towing speeds of 3–5 knots (1.54 − 2.58 m/s). The detailed videos on field-scale tests also can be found on the homepage of the KOAI Co., Ltd. (https://koai.co.kr/great-dionaea-v1/).

4.5. Collection of the floating debris (mimicking the spilled oil) in real environments

Finally, we assess the collection performance of the spilled materials in the real marine environment by using the floating debris (i.e., color foam balls) which are used to mimic the relatively large sizes of scattered oil phases in the oil spill accident site. Fig. 6d–h provides the sequential operation of tracking some floating debris from their release from Boat #1 (Fig. 6d) to their collection and inflow into the oil-water separator that is towed by Boat #2 (see supplementary movie S4). Here, the considered towing speed is 2.5 knots (1.29 m/s) at which the integrated oil-spill response system shows relatively stable operation, as shown in Fig. 6a. In the present field-scale test, we found the integrated response system has impressive maneuverability, e.g., the stable floating balance and full level of the unfolding performance (Fig. 6e and f), as well as the adequate capacity for collecting the spilled materials (Fig. 6g–i), which will make it a promising candidate to realize rapid and effective marine oil spill cleanup.

As explained, we have evaluated the feasibility and validity of the proposed system to collect, recover, and store the oil slicks from the water surface, which is expected to achieve the fast and efficient prevention and remediation at the initial stage of small oil spills. To clarify some other practical features of the present development in detail, we have compared it with existing mechanical methods in terms of the working mechanism, response stages, operational limitation, performance, benefits, and drawbacks according to previous studies (Fingas, 2002; Ventikos et al., 2004; Dhaka and Chattopadhyay, 2021) (see Table S1 in the Supplementary Materials). Based on it, the specific features of our development can be summarized as follows.

(i) The developed system has a comparable performance (recovery volume, percent oil, and recovery rate) to the conventional oil skimmers at the same operational conditions (current velocity $\lesssim$ 1.0 knots and wave height $\lesssim$ 1.5 m) but can work in faster current condition ($\sim$ 5 knots). The working mechanism of the system is the density difference/gravitational effect-driven separation, and its feature of mobile oil recovery allows it to apply in the initial physical response stage along with the mechanical containment boom/fence/curtain. This early prevention and remediation are expected to minimize the subsequent negative effects, for example, difficult recovery due to weathering processes on the sea.

(ii) In addition to the environmental factors, the performance of oil skimmers depends on the oil thickness and oil type, but the present system is affected by the towing speed and storage capacity. Unlike the usage limitation of oil skimmers in the relatively fast current condition (>1 knot), we can manipulate the towing speed and direction (lowing the inlet oil-water mixture velocity) to keep the recovery performance regardless of the type and thickness of the oil.

(iii) Since the present system is not yet commercially available, we assumed that the price of the system is comparable (or cheaper) as that of the typical oil skimmers and compared the total cost, i.e., the sum of the consumable materials and maintenance (cleaning and storage) fees. In this context, we think the cost of the present system is expected to be cheaper since it does not use the consumable (non-repeatedly useable) oleophilic surfaces (e.g., belt, disc, and rope) during the long-term use (Fingas, 2002; Dhaka and Chattopadhyay, 2021).

5. Concluding remarks

Through the series of systematic laboratory-scale experiments, meso-scale towing tank tests, and filed-scale trials, in the present study, we presented a novel marine oil-spill response system that can achieve the collection, recovery, and storage of the oil slick floating on the water surface, targeted for the initial prevention and remediation of the spill accident. Following the series of previous studies, we have already reported the detailed design and the functionalities of each compartment of the system, and the present study focused on the integration of the total system, and its validation and advancement throughout the larger-scale experiments. In the laboratory-scale experiments, first, we measured that the surface waves tend to degrade the oil-recovery rate below 80%. To sustain the effective oil recovery even in the harsh marine environment (e.g., surface waves and high-speed currents), we suggest the installation of the porous structures (e.g., mesh/net) at the inlet and water outlet of the separator. The net located at the separator inlet plays the role of wave (current) damper and that installed near the water outlet helps to maintain the stable water layer above the water outlet, which mitigates the fluctuating oil-water interface to keep the relatively higher oil-recovery rate. The results of laboratory-scale experiments show that the use of porous structures can recover the oil-recovery rate above 90% even under the high surface-wave conditions.

Further study on the scale-up (full-scale) integrated oil-spill response system was performed to evaluate its reliable collection, recovery, and storage of the oil slick in the simulated environment, i.e., towing tank tests. The oil collection part in front of the separator was optimized to have a good floating balance, assisting the collected oil to flow into the separator easily and maintaining the water layer stably above the water outlet. We also tested the oil collection with actual olive oils and bunker A fuel oil, in which the recovery rate as high as 80% (same as that measured in laboratory-scale experiments) was confirmed. Finally, the rapid deployment and stable operation of the full-scale system was tested in the actual marine environments. In addition to minimal manpower input, the system's lightweight and capability to handle different types of the spilled oil can reduce the overall time from shipping, loading/unloading, and assembly to deployment at sea. The entire response system is driven and controlled by a small boat ($\lesssim$ 10 tons) and a vane deployer; importantly, it is able to operate in a linear as well as a rotating movement at the speeds of 3–5 knots while maintaining a good floating balance and a strong sturdiness of the connection between each component.

The proposed integrated system and each component are well patented and the full-scale systems are now being dispatched to several posts of the Korea Coast Guard and tested under different situations; this is expected to bring us the quantitative analysis of the time required for oil spill detection, decision-making, and dispatch of vessels. On the other hand, it is quite promising to find out the present system can also cope with the new marine fuel oil, low sulfur fuel oil (LSFO) with a special temperature-dependent solidifying viscous behavior. Compared to other mechanical skimmers of which the performance varies significantly depending on the oil types, we believe the present system has the potential to treat the spill accidents of various oils, but it is still required to be improved to cope with the unexpected situations in practical situations, such as the viscosity increase of the spilled oil due to emulsification and fast spanwise oil spreading. In future work, we will also analyze the properties of the water released from the water outlet and explore some methods, for example, the installation of the novel oil-repellent superhydrophilic mesh (Ko et al., 2021; Lee et al., 2022a) at the water outlet to treat released water, advancing its feasibility for practical applications.

Credit author statement

Linfeng Piao: Conceptualization, Data curation, Methodology, Investigation, Writing - original draft. **Chan Jin Park**: Experiment,

Formal analysis. **Seongjin Kim**: Conceptualization. **Kyungtaek Park**: Conceptualization, Project administration, Formal analysis, Writing - review & editing. **Yongjun Lee**: Conceptualization, Formal analysis, Writing - review & editing. **Ho-Young Kim**: Conceptualization, Project administration. **Myoung-Woon Moon**: Conceptualization, Project administration, Supervision, Writing - review & editing. **Hyungmin Park**: Project administration, Supervision, Writing - review & editing.

Declaration of competing interest

The authors declare that they have no known competing financial interests or personal relationships that could have appeared to influence the work reported in this paper.

Data availability

Data will be made available on request.

Acknowledgement

This work was supported by research grants (KCG-01-2017-02 and 20210584) through the Korea Institute of Marine Science & Technology Promotion funded by Korea Coast Guard, South Korea and Institute of Engineering Research at Seoul National University, South Korea. Authors appreciate the Prof. Shin Hyung Rhee (Department of Naval Architecture and Ocean Engineering, Seoul National University), and Mr. Seung-Keun Kim and Dr. Dae-il Kim (Korea Coast Guard) for the supports for utilizing the towing-tank flow tests at the Seoul National University and Korea Coast Guard Academy, and performing the field tests in the real marine environment.

Appendix A. Supplementary data

Supplementary data to this article can be found online at https://doi.org/10.1016/j.jenvman.2023.118833.

References

Alló, M., Loureiro, M.L., 2013. Estimating a meta-damage regression model for large accidental oil spills. Ecol. Econ. 86, 167–175.
Barron, M.G., 2012. Ecological impacts of the Deepwater Horizon oil spill: implications for immunotoxicity. Toxicol. Pathol. 40, 315–320.
Behin, J., Azimi, S., 2015. Experimental and computational analysis on influence of water level on oil-water separator efficiency. Separ. Sci. Technol. 50, 1695–1700.
Bejarano, A.C., 2018. Critical review and analysis of aquatic toxicity data on oil spill dispersants. Environ. Toxicol. Chem. 37, 2989–3001.
Bullock, R.J., Aggarwal, S., Perkins, R.A., Schnabel, W., 2017. Scale-up considerations for surface collecting agent assisted in-situ burn crude oil spill response experiments in the Arctic: laboratory to field-scale investigations. J. Environ. Manag. 190, 266–273.
Cai, Q., Zhu, Z., Chen, B., Lee, K., Nedwed, T.J., Greer, C., Zhang, B., 2021. A Cross-comparison of biosurfactants as marine oil spill dispersants: governing factors, synergetic effects and fates. J. Hazard Mater. 416, 126122.
Chen, B., Ye, X., Zhang, B., Jing, L., Lee, K., 2019. Marine oil spills - preparedness and countermeasures. In: Sheppard, C. (Ed.), World Seas: an Environmental Evaluation, pp. 407–426.
Dave, D.A.E.G., Ghaly, A.E., 2011. Remediation technologies for marine oil spills: a critical review and compar- ative analysis. Am. J. Environ. Sci. 7, 423–440.
Dhaka, A., Chattopadhyay, P., 2021. A review on physical remediation techniques for treatment of marine oil spills. J. Environ. Manag. 288, 112428.
Dhanak, M.R., Xiros, N.I., 2016. Springer Handbook of Ocean Engineering. Springer.
Fingas, M., 2002. The Basics of Oil Spill Cleanup. CRC Press.
Fingas, M., 2016. Oil Spill Science and Technology. Gulf Professional Publishing, Cambridge.
Ivshina, I.B., Kuyukina, M.S., Krivoruchko, A.V., Elkin, A.A., Makarov, S.O., Cunningham, C.J., Peshkur, T.A., Atlas, R.M., Philp, J.C., 2015. Oil spill problems and sustainable response strategies through new technologies. Environ. Sci. Process. Impacts 17, 1201–1219.
Ko, T.-J., Cho, S., Kim, S.J., Lee, Y.A., Kim, D.H., Jo, W., Kim, H.-Y., Yang, S., Oh, K.W., Moon, M.-W., 2021. Direct recovery of spilled oil using hierarchically porous oil scoop with capillary-induced anti-oil-fouling. J. Hazard Mater. 410, 124549.
Lee, Y.A., Cho, S., Choi, S., Kwon, O.C., Yoon, S.M., Kim, S.J., Park, K.-C., Chung, S., Moon, M.W., 2022a. Slippery, water-infused membrane with grooved nanotrichomes for lubricating-induced oil repellency. Adv. Sci. 9, 2103950.
Lee, Y.A., Park, Y.C., Kwon, O., Kim, S.J., Chung, S., Moon, M.W., 2022b. Hygroscopic ramie fabrics for recovering highly viscous low sulfur fuel oil. Environ. Pollut. 308, 119668.
Lee, J., Piao, L., Park, H., 2023. Characterization of the physical and weathering properties of low sulfur fuel oil (LSFO) and its spreading on water surface. J. Hazard Mater. 453, 131444.
Lessard, R.R., DeMarco, G., 2000. The significance of oil spill dispersants. Spill Sci. Technol. Bull. 6, 59–68.
Michel, J., Fingas, M., 2016. Oil Spills: causes, consequences, prevention, and countermeasures. In: Fossil Fuels: Current Status and Future Directions, pp. 159–201.
Ossai, I.C., Ahmed, A., Hassan, A., Hamid, F.S., 2020. Remediation of soil and water contaminated with petroleum hydrocarbon: a review. Environ. Technol. Innov. 17, 100526.
Park, J., Park, H., 2019. Vane deployer with a hydrofoil array for enhanced lift-to-drag ratio at wide range of angle of attack. J. Korean Soc. Vis. 17, 25–31.
Park, J., Seo, J., Lee, S.B., Rhee, S.H., 2022. Turbulence structure under the free-surface wave around an advancing surface-piercing cylindrical body. Phys. Fluids 34, 123311.
Piao, L., Park, H., 2019. Relation between oil-water interfacial flow structure and their separation in the oil-water mixture flow in a curved channel: an experimental study. Int. J. Multiphas. Flow 120, 103089.
Piao, L., Park, H., 2021. Interfacial instability for droplet formation in two-layer immiscible liquids under rotational oscillation. J. Fluid Mech. 924, A32.
Piao, L., Kim, N., Park, H., 2017. Effects of geometrical parameters of an oil-water separator on the oil-recovery rate. J. Mech. Sci. Technol. 31, 2829–2837.
Sandifer, P.A., Ferguson, A., Finucane, M.L., Partyka, M., Solo-Gabriele, H.M., Walker, A. H., Wowk, K., Caffey, R., Yoskowitz, D., 2021. Human health and socioeconomic effects of the Deepwater Horizon oil spill in the Gulf of Mexico. Oceanography 34, 174–191.
Schnurr, R.E., Walker, T.R., 2019. Marine transportation and energy use. In: Reference Module in Earth Systems and Environmental Sciences. Elsevier, Amsterdam, The Netherlands, pp. 1–9.
Si-Zhong, Y., Hui-Jun, J.I.N., Zhi, W.E.I., Rui-Xia, H.E., Yan-Jun, J.I., Xiu-Mei, L.I., Shao-Peng, Y.U., 2009. Bioremediation of oil spills in cold environments: a review. Pedosphere 19, 371–381.
Uhler, A.D., Stout, S.A., Douglas, G.S., Healey, E.M., Emsbo-Mattingly, S.D., 2016. Chemical character of marine heavy fuel oils and lubricants. In: Standard Handbook Oil Spill Environmental Forensics. Academic Press, pp. 641–683.
Ventikos, N.P., Vergetis, E., Psaraftis, H.N., Triantafyllou, G., 2004. A high-level synthesis of oil spill response equipment and countermeasures. J. Hazard Mater. 107, 51–58.